

Antibacterial Adhesion of Poly(methyl methacrylate) Modified by Borneol Acrylate

Xueli Sun,[†] Zhiyong Qian,^{‡,§} Lingqiong Luo,[†] Qipeng Yuan,[†] Ximin Guo,^{‡,§} Lei Tao,^{||} Yen Wei,^{||} and Xing Wang^{*,†}

[†]Beijing Laboratory of Biomedical Materials, Beijing University of Chemical Technology, Beijing 100029, P. R. China

[‡]Key Laboratory for Biomechanics and Mechanobiology of Ministry of Education, School of Biological Science and Medical Engineering, Beihang University, Beijing 100191, P. R. China

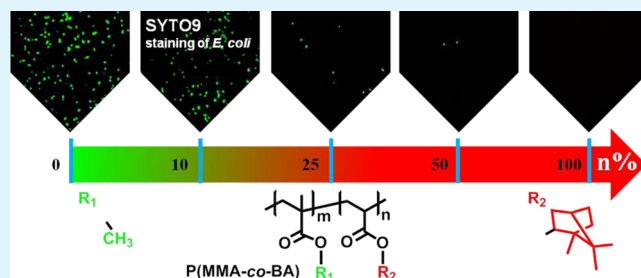
[§]Department of Advanced Interdisciplinary Studies, Institute of Basic Medical Sciences, Beijing 100850, P. R. China

^{||}Department of Chemistry, Tsinghua University, Beijing 100084, P. R. China

S Supporting Information

ABSTRACT: Poly(methyl methacrylate) (PMMA) is a widely used biomaterial. But there is still a challenge facing its unwanted bacterial adhesion because the subsequent biofilm formation usually leads to failure of related implants. Herein, we present a borneol-modified PMMA based on a facile and effective stereochemical strategy, generating antibacterial copolymer named as P(MMA-co-BA). It was synthesized by free radical polymerization and studied with different ratio between methyl methacrylate (MMA) and borneol acrylate (BA) monomers. NMR, GPC, and EA, etc., were used to confirm their chemical features. Their films were challenged with *Escherichia coli* (Gram-negative) and *Bacillus subtilis* (Gram-positive), showing a BA content dependent antibacterial performance. The minimum effective dose should be 10%. Then *in vivo* subcutaneous implantations in mice demonstrated their biocompatibilities through routine histotomy and HE staining. Therefore, P(MMA-co-BA)s not only exhibited their unique antibacterial character but also suggested a potential for the safe usage of borneol-modified PMMA frame and devices for further implantation.

KEYWORDS: antibacterial adhesion, poly(methyl methacrylate), borneol, copolymer, implant



1. INTRODUCTION

Poly(methyl methacrylate) (PMMA) has been widely applied in healthcare due to their unique properties, such as high flexibility, ease of fabrication, acceptable biocompatibility, and physical and chemical stability.^{1,2} It is well-known as the main composition of organic glass cranioplasty materials,³ bone cement for false teeth,^{4,5} prosthesis,⁶ and contact lenses.⁷ Although those PMMA implants has been demonstrated to be appropriate for *in vivo* usage, scientists or surgeons have still been paying much attention to their antibacterial modification, owing to the frequent occurrence of bacterial infection and implants failure.⁸

Previous studies demonstrated that antibacterial agents (organic or inorganic) could be introduced into PMMA for its antibacterial modification. As a general strategy, Jang's group reported the PMMA-Ag nanofiber with good antibacterial efficacy.⁹ Carmona-Ribeiro et al. showed that quaternary ammonium modified PMMA displayed remarkable antimicrobial activity.^{10,11} Meanwhile, striving for excellence has never stopped.¹²⁻¹⁴ However, all those antibacterial agents used in PMMA might increase the risks of developing drug resistance bacteria and the potential toxicity on human and environment.^{15,16} Therefore, a new strategy is highly desired.

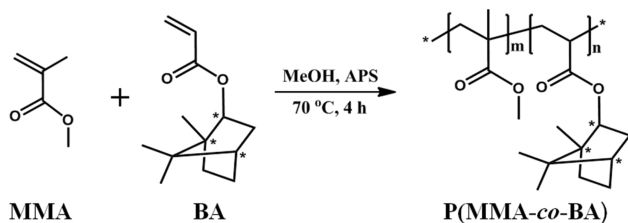
Recently, our group has successfully developed a series of borneol-based polymers (PBAs) that showed unique antibacterial adhesion properties by dramatically reducing bacterial attachment and biofilm formation.¹⁷ It is believed that the antibacterial activity is resulted from the complex molecular structure of borneol isomers on the materials surface compared with the simple methyl of PMMA control. This proof-of-concept demonstration thus suggested that utilizing polymer surface stereochemistry is an advanced strategy for antimicrobial adhesion. As an example, the borneol-grafted cellulose (BGC) has been further prepared,¹⁸ and this modification resulted in a successful conversion of the antifungal activity from surrender of natural cellulose into remarkable resistance of BGC (antifungal adhesion and fungal growth inhibition). Therefore, above works not only suggested that the grafted borneol moieties are crucial for influencing the tactile sensing of microbes and their subsequent selective inadhension behaviors but also inspired us to modify conventional biomedical polymers for their antimicrobial applications.

Received: August 21, 2016

Accepted: October 7, 2016

Herein, by employing MMA and BA monomers in different ratios, we aim to make copolymers (Scheme 1) with a facile

Scheme 1. Route for Synthesis of the Antibacterial Copolymer Named as P(MMA-co-BA)^a



^aThose copolymers are denoted as P_x in this study, where $x = 0, 10, 25, 50,$ and $100,$ respectively, meaning mole percent of BA units and corresponding to the designed mole ratio of $n = 0, m:n = 9:1, m:n = 3:1, m:n = 1:1,$ and $m = 0,$ respectively.

method of free radical polymerization and to investigate how the content of BA units affect overall antibacterial properties of the as-synthesized P(MMA-co-BA)s. In addition, we try to find what is the minimal effective mole percent for the copolymerized BA units in this P(MMA-co-BA) system through challenging both Gram-negative *Escherichia coli* (*E. coli*) and Gram-positive *Bacillus subtilis* (*B. subtilis*) bacteria. Furthermore, those P(MMA-co-BA)s will be evaluated with *in vivo* subcutaneous implantations in mice to answer whether this modification is a feasible strategy for forming biocompatible copolymers. In addition, a comparison between the P(MMA-co-BA)s and zwitterionic compounds,^{19–21} known as good biomaterials with antibacterial activity and acceptable biocompatibility *in vivo*, is also discussed.

2. EXPERIMENTAL SECTION

2.1. Materials. Isobornyl acrylate (BA, 93%) was purchased from Sigma-Aldrich Company. Methyl methacrylate (MMA, 98%), methanol (CH₃OH, 99.9%), dichloromethane (CH₂Cl₂, 99%), and ammonium persulfate ((NH₄)₂S₂O₈, 98%) were obtained from Tokyo Chemical Industry (TCI). Sulfuric acid (H₂SO₄, 98%), hydrogen peroxide (H₂O₂, 30%), tetrahydrofuran (THF, 99.9%), chloroform-*d* (CDCl₃, 99.99%), and dimethyl sulfoxide (DMSO, 99.7%) were purchased from J&K Scientific. 3-(4,5-Dimethyldiazol-2-yl)-2,5-diphenyltetrazolium bromide (MTT) was purchased from Simcere. Sodium chloride (NaCl, 99%), peptone (BR), beef extract (BR), and agar (BR) were purchased from Aladdin. The BacLight live/dead kit (Molecular Probes) was purchased from Thermo Fisher Scientific. Gram-positive bacteria (*B. subtilis*, ATCC 9372) and Gram-negative bacteria (*E. coli*, ATCC 25922) were obtained from China Center of Industrial Culture Collection and were incubated at 37 °C on a nutrient agar plate for 24 h before use.

2.2. Copolymer Synthesis and Characterization. The synthesis of the copolymers, denoted as P_x ($x = 0, 10, 25, 50,$ and $100,$ meaning mole percent of BA units), was carried out in a 10 mL penicillin bottle. A typical synthesis procedure of P₁₀ was as follows: first, MMA (620 mg, 6.19 mmol) and BA (135 mg, 0.65 mmol) monomers were dissolved in 800 μL of degassed methanol with the mole ratio of 9:1; then 148 μL of ammonium persulfate (0.1 g mL⁻¹ of water solution) as an initiator was added into the solution and shook well; after that it was heated at 70 °C for 4 h. The obtained solid was further purified by alternate treatments with dichloromethane (dissolution) and methanol (precipitate). The product was obtained as a white solid with a yield of 92%. These bulk copolymers were used to prepare copolymer films.

The copolymers were characterized with gel permeation chromatography (GPC), water contact angle (CA), elemental analysis (EA),^{22,23} and nuclear magnetic resonance spectroscopy (¹H

NMR).²⁴ GPC was performed on a Waters 1515 GPC. CA was performed on a JC2000D3. EA was measured with a VARIO EL cube. ¹H NMR spectra were recorded on a Bruker AV III 400 spectrometer using CDCl₃ as the solvent. Moreover, *in vitro* degradation of P(MMA-co-BA)s (20 mm diameter with a thickness of 5 mm) was investigated during a 4-week period in PBS (pH 7.4) at 37 °C.

2.3. Antibacterial Adhesion Tests. A single colony (strains of *E. coli* or *B. subtilis*) was picked into 50 mL of sterile beef-protein liquid medium, in which peptone, beef extract, and NaCl were dissolved in deionized water at pH 7. After that they were cultured overnight at 37 °C, with a shaking rate of 200 rpm. Finally, bacteria solutions were diluted to a concentration of 10⁶ CFU mL⁻¹ (colony-forming unit) with sterile saline solution.

The modified “prison break” experiment was performed to study interactions between bacteria and P(MMA-co-BA)s. Five circular P_x films (P₀, P₁₀, P₂₅, P₅₀, and P₁₀₀) were sterilized under ultraviolet light and fixed onto beef-protein medium. After that five small circular sterile media were fixed onto those copolymer films, forming sandwich structures. 2 μL of *E. coli* suspension (10⁶ CFU mL⁻¹) was added on each of the small circular media and cultured at 37 °C. The results at different time points were recorded by a camera. For this evaluation, each experiment was repeated at least three times.

The plate count methods^{25,26} was used to study the antibacterial performance of P(MMA-co-BA)s. First, each sterilized P_x film (1 cm diameter) was used to contact with 100 μL of *E. coli* suspension (10⁶ CFU mL⁻¹) for 1 or 24 h. Second, after rinsing gently with sterile water three times, bacteria adhered on the surface of P_x film were dispersed into 5 mL of sterile water by using an ultrasonic cleaner. Finally, a 100 μL dispersion was coated on beef-protein medium and further cultured for 24 h at 37 °C. The numbers of *E. coli* colonies were counted.

In the same way, optical density (OD) testing²⁷ was also performed. After the step of gently rinsing, P_x films were incubated in 50 mL of sterile LB (Luria–Bertani) medium and cultured with shaking (200 rpm) at 37 °C. *E. coli* outgrowth was estimated by monitoring the OD changes at 600 nm.

2.4. In Situ Biofilm Prevention Assay. Antibacterial activity of the copolymers was determined by MTT metabolic assay.^{28,29} First, each sterilized P_x film (1 cm diameter) was used to contact with 100 μL of *E. coli* suspension (10⁶ CFU mL⁻¹) for 1 or 24 h. After rinsing gently, all P_x films were transferred to a 96-well plate for MTT assay (repeat three wells for each P_x film). Briefly, one P_x film was placed in a well and inoculated with 100 μL of MTT (5 mg mL⁻¹). They were cultured at 37 °C for 4 h without light. Then, the MTT solution was removed, and the plate were incubated for 10 min with a solution of DMSO (150 μL) for each well to dissolve the formazan product. The absorbance at 540 nm was measured via a microplate reader (PT-3502G). A higher absorbance indicates a higher formazan concentration, which in turn indicates more metabolic activity of the bacteria on the film.

The BacLight live/dead fluorescent assay^{30,31} was used to investigate the bacterial attachment onto P_x films. First, each film was incubated with 3 mL of bacterial suspension (10⁷ CFU mL⁻¹) at 4 °C for 4 h. Then, P_x films were washed three times with sterile sodium chloride solution. All the films were stained using the BacLight live/dead kit (Molecular Probes, Eugene, OR). Live bacteria were stained with SYTO9 to produce green fluorescence, and bacteria with compromised membranes were stained with PI to produce red fluorescence. The films were examined using an inverted epifluorescence microscope, and finally the images were recorded.

2.5. In Vivo Biological Evaluation. Male Kunming mice (weighing 22–24 g) were housed in sterilized cages and fed standard pellets and water ad libitum. 40 mice were employed for implantation (four mice for each time point), and each mice implanted with two P_x films. Before implantation, P_x films were cut into squares (approximately 1 × 1 cm with a thickness of 300 μm) and sterilized by γ-irradiation (25 kGy). The surgical instruments were sterilized by autoclaving. The mice were anaesthetized with 2% (w/w) pentobarbital sodium prior to the operation. Then, the hair on the mice dorsum were shaved and sterilized with 75% ethanol and PI. An

incision (approximately 1.5 cm) on each side of the dorsum was made using a scalpel. Next, subcutaneous pouches were created in the incisions using vessel forceps, and P_x films were implanted into each pocket. After implantation, the wounds were sutured.

The mice were sacrificed by cervical dislocation at specific time points (7 and 28 days) after surgery. The tissues associated with and adjacent to the copolymer films were harvested using a scalpel. The results at different time points were recorded by a camera. Then, P_x films with the surrounding tissue (approximately 1 × 1 cm) were fixed in 4% paraformaldehyde for histology.

Prior to being embedded in paraffin wax, the samples (a thickness of 5 μm) were dehydrated using a graded series of alcohol (50, 70, 80, 95, and 100%). The xylene was used to make the organization transparent. The copolymers were found to solved in this treatment. Then, the samples were embedded in paraffin, sectioned using a microtome (Leica RM2016, Leica Microsystems, Germany), and stained with hematoxylin and eosin (HE). The samples were viewed and recorded using light microscopy in the region around the implants. Tissue inflammatory responses were then evaluated.^{32,33}

3. RESULTS AND DISCUSSION

3.1. Copolymer Characterization. GPC was first performed to test the copolymers (Figure S1). Table S1 (see Supporting Information) lists their molecular weight (both M_n and M_w) in the range of 10^4 – 10^5 g mol⁻¹ with polydispersity index (PDI) of 1.8–3.7. They are acceptable for a simple thermal polymerization of bulk copolymer synthesis. Figure 1a

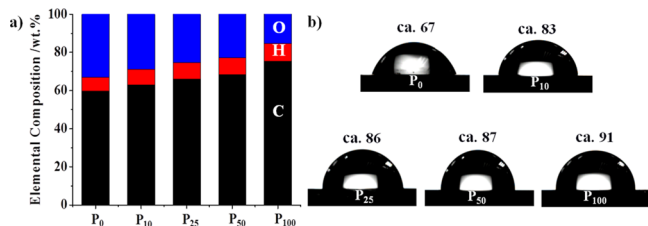


Figure 1. (a) EA tests of P_x copolymers. (b) CA measurements on P_x films. Data values corresponded to mean ± SD ($n = 3$).

shows the EA results of P(MMA-*co*-BA)s. Since BA unit has a large C₁₀ carbon group, carbon content increases by degrees with the increasing of BA units, resulting in a progressive increment from 59.79% to 75.25%. In contrast, oxygen content in P(MMA-*co*-BA)s gradually decreased. These changings met our expectations that BA have incorporated with MMA successfully. Since BA has a large hydrophobic carbon cage structure, CA measurements were also used to check the copolymers. When BA units increased in P(MMA-*co*-BA)s, the water CA should become hydrophobic gradually. Figure 1b shows that pure PMMA (P₀) surface has a water CA of $67 \pm 3^\circ$, while PBA displays a water CA of $91 \pm 2^\circ$. When P(MMA-*co*-BA)s were measured in the sequence of P₁₀, P₂₅, and P₅₀, the water CA of those copolymers exhibited a hydrophobic enhancement in the order of $83 \pm 1^\circ$, $86 \pm 3^\circ$, and $87 \pm 1^\circ$, respectively. This phenomenon can be attributed to the regular increasing of BA units on the copolymers surfaces.

Further quantitative analysis was performed by ¹H NMR detection (Figure 2). For the homopolymer PMMA (Figure 2, P₀), the peak at $\delta = 3.68$ was assigned to the characteristic peak of the denoted methyl ester group (x in Figure 2);³⁴ while for the homopolymer PBA (Figure 2, P₁₀₀), the assigned peak at $\delta = 4.65$ was used to represent the borneol group (y in Figure 2). Therefore, within the spectra of P₁₀, P₂₅, and P₅₀, the integral area ratio of above-mentioned two peaks can be calculated

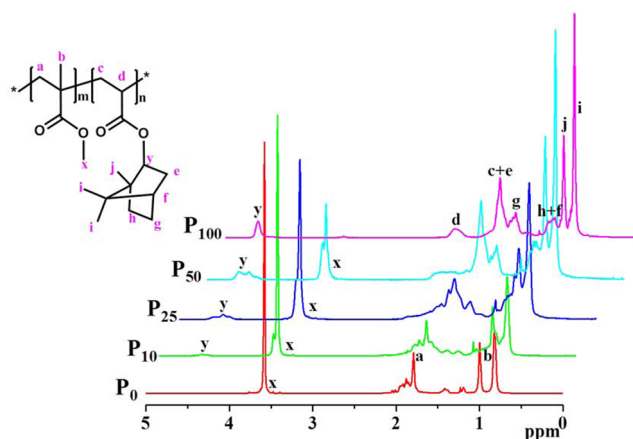


Figure 2. ¹H NMR spectra of P(MMA-*co*-BA)s: P₀, P₁₀, P₂₅, P₅₀, and P₁₀₀.

(Table S2 in Supporting Information), where the actual mole percent from 9.6% to 28% and further to 53% is similar to our design. Anyway, the denoted P_x is still used to describe the characteristic P(MMA-*co*-BA)s below.

3.2. Antibacterial Adhesion Tests. To evaluate the antibacterial activities of P(MMA-*co*-BA)s, a visualized method, modified “prison break” experiment (Figure 3a), is designed to observe the antibacterial adhesion capability of the copolymers. A sandwich construction, rather than a polymer ring,¹⁷ is used

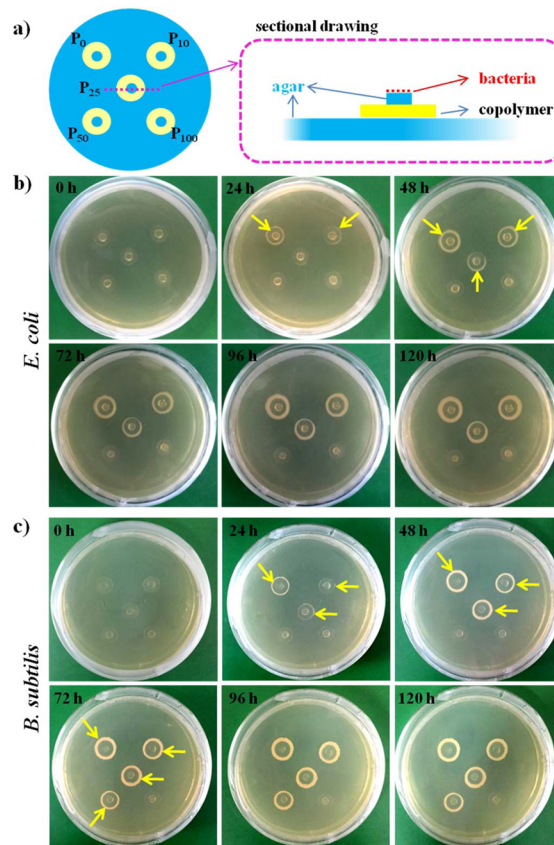


Figure 3. (a) Schematic illustration of a modified “prison break” experiment for antibacterial adhesion assay of polymer film. Controlling the escape of (b) *E. coli* and (c) *B. subtilis* from P_x films was recorded at denoted periods (0, 24, 48, 72, 96, and 120 h).

here handily. Figure 3b shows that P(MMA-co-BA)s films can efficiently inhibit the expanding growth of Gram-negative *E. coli*. In the first 24 h, *E. coli* succeeded in breaking the restrictions of P₀ film to diffuse outside. P₁₀ film could not completely restrict the outward spread of *E. coli*, although relatively less *E. coli* was found there. Compared with P₀ film, P₁₀ film has slightly improved its antibacterial adhesion capability. Meanwhile, P₂₅, P₅₀, and P₁₀₀ films displayed good restriction for the spread out of *E. coli*. After 48 h, P₂₅ film was broke; meanwhile, *E. coli* at the outer of both P₀ and P₁₀ films were growing up. But, P₅₀ and P₁₀₀ films still exhibited excellent restrictive for *E. coli*, which could not break the “copolymer prison” even after 120 h. These phenomena indicated that increasing BA units (from 9.6% to 28% and further to 53%, actually; see details in the Supporting Information) led to a gradually higher antibacterial efficacy. When BA units increased to over 50%, antibacterial performance of the copolymers was similar to pure PBA.

In addition, Gram-positive *B. subtilis* was chosen as model bacteria to challenge P_x films (Figure 3c). In the first 24 h, *B. subtilis* succeeded in breaking the restrictions of P₀ film as well as *E. coli*. Differently, P₁₀ and P₂₅ films have also been broken by *B. subtilis* within 24 h through careful observation. These evidences were confirmed after 48 h. Furthermore, P₅₀ film kept its antibacterial effect more than 48 h, but less than 72 h; P₁₀₀ film showed excellent restrictive for *B. subtilis* more than 120 h. These results suggested that increasing BA units contributed significant improvement for the copolymers' antibacterial activity, though *B. subtilis* displayed more powerful fouling capacity than *E. coli*. Nevertheless, P(MMA-co-BA)s have a broad spectrum of antibacterial adhesion.

Besides the macro-observation, we further scanned the uncovered areas of those copolymer films from their inner to outer edges by utilizing an optical microscope (Figure S3). The P₀ film showed a high density of *B. subtilis* either inside or outside of the exposed polymer rings. For other copolymers, with the increase of BA units, *B. subtilis* gradually reduced their coverage area and especially from inside to outside. Remarkably, only sporadic *B. subtilis* was found inside of P₁₀₀ film; almost no *B. subtilis* was observed when the checked region extended to outside of the film. Therefore, the typical pattern of *B. subtilis* coverage versus BA content of P(MMA-co-BA)s further confirmed the reinforced antibacterial performance of the borneol modified copolymers.

Antibacterial activities of all P(MMA-co-BA)s were also investigated by classical methods.^{17,27} Figure 4a shows the plate count results of those copolymers. The number of single *E. coli* colonies of P₀ film (1033 units) is about 10 times higher than that of P₁₀ film (114 units), nearly 130 times higher than that of P₂₅ film (8 units), and more than 1000 times higher than that of P₅₀ and P₁₀₀ films (1 unit). It is clear that BA units contribute greatly for the antibacterial property of those copolymers. 10% of BA addition has displayed a distinct inhibition on bacterial adhesion. When the content of BA units is up to 50%, the antibacterial activity has nearly approached to that of pure PBA polymer.

The optical density (OD) test was also performed to verify above-mentioned regularity. As shown in Figure 4b, the specific densities were found among the five test groups of P_x after 9 h of incubation, when *E. coli* has just lived through a lag phase and coming into a logarithmic phase of bacterial reproduction. Particularly after 10.5 h of incubation, the broths exhibited intuitive turbidities among the five bacterial suspensions

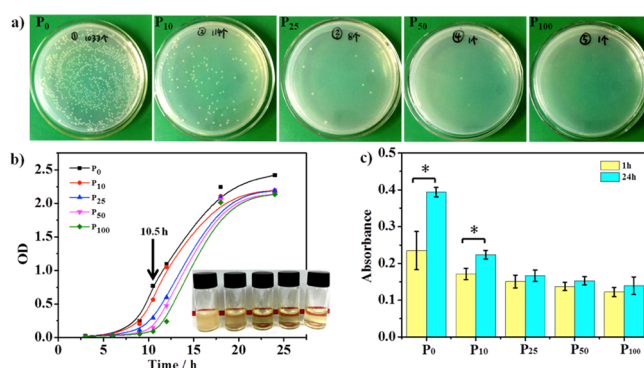


Figure 4. (a) Plate count experiments of *E. coli*. Colony numbers corresponding to viable *E. coli* on P₀, P₁₀, P₂₅, P₅₀, and P₁₀₀ films were 1033, 114, 8, 1, and 1 units, respectively. (b) OD₆₀₀ test for evaluating interactions between *E. coli* and P_x films. For above two tests, P_x films were soaked in an *E. coli* suspension for 1 h. (c) Metabolic activity of *E. coli* adhered on P_x films after 1 and 24 h coincubation. It was measured via the MTT assay. Data values corresponded to mean ± SD (*n* = 3); **P* < 0.05.

(Figure 4b, inset), where the P₀ test group was opaque, the P₁₀ test group was translucent, and the P₂₅, P₅₀, and P₁₀₀ test groups were relatively clear. In addition, even contacting with *E. coli* for 24 h, as shown in Figures S4 and S5, similar regularity was observed for those P(MMA-co-BA)s.

In order to demonstrate the above-mentioned antibacterial properties *in situ*, MTT assay was further employed within different periods.^{28,29} Briefly, P_x films were incubated with *E. coli* for 1 and 24 h. Then the live bacteria on P_x films were determined by the MTT assay at 540 nm. Figure 4c shows a distinct decrease of absorbance following the sequence of P_x films for the two periods of time. Only on P₀ and P₁₀ surfaces, a statistically significant difference happened, meaning that bacteria reproduced there to a certain degree (69% for P₀; 31% for P₁₀). However, on the surfaces of P₂₅, P₅₀, and P₁₀₀ films, no statistical difference could be found. These *in situ* results are well consistent with aforementioned methods.

However, how many dead bacteria on this kind of copolymer's surface is still unknown, since MTT assay is only related to live cells *in situ*. Therefore, *in situ* fluorescent live/dead straining was carried out on P_x films. After 4 h of interaction between P_x films and *E. coli*, SYTO9/PI was stained on the surfaces of P_x films (Figure 5). Compared with P₀ (unmodified PMMA), the bacterial population (green fluorescence of SYTO9 staining in Figure 5a) reduced dramatically on the surfaces from P₁₀ to P₁₀₀. In particular, P₁₀₀ reduced 99.7% of *E. coli* adhesion. At the same time, only sporadic dead bacteria (red fluorescence of PI staining in Figure 5a) could be found on all the surfaces. Figure 5b lists the quantitative data for live/dead bacterial count. Compared with the live cells, the dead cells are almost negligible. Thus, it not only proved that this kind of copolymer has a capability of antibacterial adhesion but also confirmed that the activity is mainly due to initial sensing and subsequent selection of reversible bacterial attachment, relating interfacial stereochemistry of borneol-grafted copolymers, rather than normal mechanism of killing or virulence.

3.3. In Vivo Biocompatibility. Considering the application potential as implants of these copolymers, *in vivo* biocompatibility of P_x films (1 × 1 cm with a thickness of 300 μm) were evaluated using a mice subcutaneous implantation model.

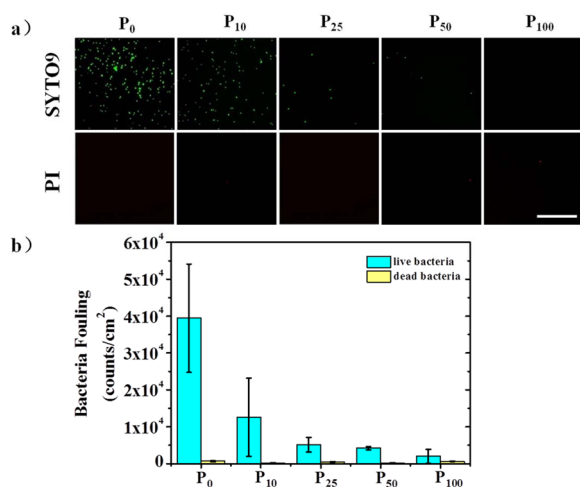


Figure 5. Bacterial adhesion tests on Px films. (a) Typical fluorescence microscopy images of attached *E. coli* cells from a suspension of 10^7 cells mL^{-1} after exposure to various films for 4 h. The live *E. coli* cells are stained green, while the dead cells are stained red. The scale bars in the images are $20 \mu\text{m}$. (b) Quantitative results for bacterial adsorption on Px films. They were estimated using ImageJ software. Data values corresponded to mean \pm SD ($n = 3$).

During experiments, all of the mice survived without any complications, and no inflammatory response or necrosis was observed in implantation areas (Figure 6), both for a short

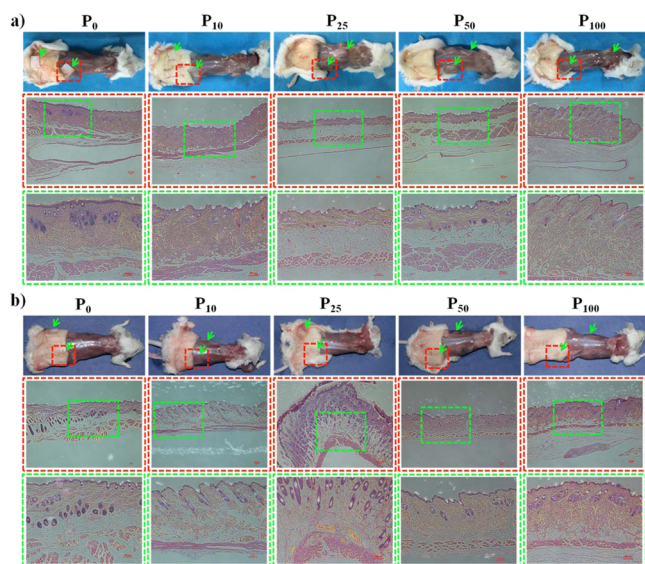


Figure 6. Histological analysis of tissues after 7 days (a) and 28 days (b) of subcutaneous implantation of Px slices (green arrows) in mice ($n = 4$). The typical HE staining is used for histological observation.

period (7 days) and for a long period (28 days). All histological sections were collected after the denoted period. Figure 6a shows images of HE stained sections of Px implants after implantation for 7 days. In all five groups of implants, connective tissue (stained pink) was exhibited with clear tissue profile and in close contact with the copolymer film. From the enlarged images, we could not find any inflammatory cell, necrotic cell, macrophage fusion into foreign body giant cell, and fibroblast activation. Even after 28 days as shown in Figure 6b, still normal tissue morphologies were detected in the tissue slices, except that the copolymer implants have partially

degraded (see Figure S2 for the *in vitro* degradation test). But at least, this case did not trigger the innate immune system of host to generate any inflammatory response to the surrounding tissue cells, as no obvious inflammation or foreign body reaction was observed there. These results unequivocally demonstrated that this kind of copolymer has very good biocompatibility. Therefore, those copolymers appear to be well suited to act as tissue implants.^{32,33}

A major advantage of P(MMA-co-BA)s over traditional antibacterial materials, antibiotics-releasing composites in particular, is their no chance to develop resistance that has been considered as a serious worldwide problem nowadays. Therefore, as one of those advanced antibacterial strategies such as zwitterionic compounds,^{19–21,35} covalent grafting of functional agents and their composite,^{35–38} this stereochemistry strategy should be a new opportunity to modify biomedical materials and interfaces owing to their good biocompatibility. However, the antibacterial performance of P(MMA-co-BA)s may be considered to be decreasing over time due to its inability of kill bacteria. But in fact, in the surgical environment, sterile operation is required. Thus, only tiny amounts of bacteria have opportunity to attach on material surfaces. Unlike PMMA that is bacterial affinity, P(MMA-co-BA)s could prevent potential bacterial adhesion for a reasonable period when the body's own immune system might fight off nonadherent bacteria. As evidence or proof, all of those implants in mice did not occur any inflection within both short and long test periods (Figure 6).

4. CONCLUSION

In summary, we developed a novel copolymer P(MMA-co-BA) that can effectively prevent bacterial adhesion. No less than 10% of BA segments can evoke distinct antibacterial activity, and up to 25% of BA segments may endow this copolymer outstanding antibacterial performance, which is close to the pure PBA that can reduce 99.7% of *E. coli* adhesion compared with unmodified PMMA surface. If extending the durable time of this copolymer to a longer scale, more percent of BA segments should be employed. Potentially, for the purpose of acting as implants, *in vivo* evaluation of subcutaneous implantation in mice has provided a certain reference for the safe use of P(MMA-co-BA)s. It strongly suggested that P(MMA-co-BA)s are biocompatible copolymers. Therefore, this strategy is a simple, efficient, and feasible method to generate bioaffinity and environmentally benign biomaterials and interfaces, especially for the prevention of bacterial colonization in biomedical devices and applications.³⁹

■ ASSOCIATED CONTENT

Supporting Information

The Supporting Information is available free of charge on the ACS Publications website at DOI: 10.1021/acsami.6b10498.

GPC results, NMR calculation, *in vitro* degradation of copolymers, optical micrographs of *B. subtilis*, plate count experiments, and OD tests at 24 h (PDF)

■ AUTHOR INFORMATION

Corresponding Author

*E-mail: wangxing@mail.buct.edu.cn (X.W.).

Author Contributions

X.S. and Z.Q. contributed equally to this work.

Notes

The authors declare no competing financial interest.

ACKNOWLEDGMENTS

The authors thank the National Natural Science Foundation of China (21204004, 21574008), the Fundamental Research Funds for Central Universities of China (YS1407), and the BUUCT Fund for Disciplines Construction and Development (XK1538) for their financial support.

REFERENCES

- (1) Jacobs, E.; Saralidze, K.; Roth, A. K.; de Jong, J. J. A.; van den Bergh, J. P. W.; Lataster, A.; Brans, B. T.; Knetsch, M. L. W.; Djordjevic, I.; Willems, P. C.; Koole, L. H. Synthesis and Characterization of a New Vertebroplasty Cement Based on Gold-Containing PMMA Microspheres. *Biomaterials* **2016**, *82*, 60–70.
- (2) Saha, S.; Pal, S. Mechanical Properties of Bone Cement: A Review. *J. Biomed. Mater. Res.* **1984**, *18*, 435–462.
- (3) Itokawa, H.; Hiraide, T.; Moriya, M.; Fujimoto, M.; Nagashima, G.; Suzuki, R.; Fujimoto, T. A 12 Month in Vivo Study on the Response of Bone to a Hydroxyapatite–Polymethylmethacrylate Cranioplasty Composite. *Biomaterials* **2007**, *28*, 4922–4927.
- (4) Tan, H.; Peng, Z.; Li, Q.; Xu, X.; Guo, S.; Tang, T. The Use of Quaternised Chitosan-Loaded PMMA to Inhibit Biofilm Formation and Downregulate the Virulence-Associated Gene Expression of Antibiotic-Resistant *Staphylococcus*. *Biomaterials* **2012**, *33*, 365–377.
- (5) Yi, L.; Jin, C.; Wang, L.; Liu, J. Liquid-Solid Phase Transition Alloy as Reversible and Rapid Molding Bone Cement. *Biomaterials* **2014**, *35*, 9789–9801.
- (6) Shome, D.; Honavar, S. G.; Raizada, K.; Raizada, D. Implant and Prosthesis Movement after Enucleation: A Randomized Controlled Trial. *Ophthalmology* **2010**, *117*, 1638–1644.
- (7) Li, S.; Toprak, M. S.; Jo, Y. S.; Dobson, J.; Kim, D. K.; Muhammed, M. Bulk Synthesis of Transparent and Homogeneous Polymeric Hybrid Materials with ZnO Quantum Dots and PMMA. *Adv. Mater.* **2007**, *19*, 4347–4352.
- (8) Neoh, K. G.; Hu, X.; Zheng, D.; Kang, E. T. Balancing Osteoblast Functions and Bacterial Adhesion on Functionalized Titanium Surfaces. *Biomaterials* **2012**, *33*, 2813–2822.
- (9) Kong, H.; Jang, J. Antibacterial Properties of Novel Poly(methyl methacrylate) Nanofiber Containing Silver Nanoparticles. *Langmuir* **2008**, *24*, 2051–2056.
- (10) Melo, L. D.; Palombo, R. R.; Petri, D. F. S.; Bruns, M.; Pereira, E. M. A.; Carmona-Ribeiro, A. M. Structure-Activity Relationship for Quaternary Ammonium Compounds Hybridized with Poly(methyl methacrylate). *ACS Appl. Mater. Interfaces* **2011**, *3*, 1933–1939.
- (11) Naves, A. F.; Palombo, R. R.; Carrasco, L. D. M.; Carmona-Ribeiro, A. M. Antimicrobial Particles from Emulsion Polymerization of Methyl Methacrylate in the Presence of Quaternary Ammonium Surfactants. *Langmuir* **2013**, *29*, 9677–9684.
- (12) Aly, M. A. S.; Gauthier, M.; Yeow, J. On-Chip Cell Lysis by Antibacterial Non-Leaching Reusable Quaternary Ammonium Monolithic Column. *Biomed. Microdevices* **2016**, *18*, 2.
- (13) Liu, S.; Tonggu, L.; Niu, L.; Gong, S.; Fan, B.; Wang, L.; Zhao, J.; Huang, C.; Pashley, D. H.; Tay, F. R. Antimicrobial Activity of a Quaternary Ammonium Methacryloxy Silicate-Containing Acrylic Resin: A Randomised Clinical Trial. *Sci. Rep.* **2016**, *6*, 21882.
- (14) Natarajan, S.; Kumari, J.; Lakshmi, D. S.; Mathur, A.; Bhuvaneshwari, M.; Parashar, A.; Pulimi, M.; Chandrasekaran, N.; Mukherjee, A. Differences in Antibacterial Activity of PMMA/TiO₂/Ag Nanocomposite on Individual Dominant Bacterial Isolates from Packaged Drinking Water, and Their Consortium under UVC and Dark Conditions. *Appl. Surf. Sci.* **2016**, *362*, 93–101.
- (15) Banerjee, I.; Pangule, R. C.; Kane, R. S. Antifouling Coatings: Recent Developments in the Design of Surfaces That Prevent Fouling by Proteins, Bacteria, and Marine Organisms. *Adv. Mater.* **2011**, *23*, 690–718.
- (16) Arciola, C. R.; Campoccia, D.; Montanaro, L. Effects on Antibiotic Resistance of *Staphylococcus epidermidis* Following Adhesion to Polymethylmethacrylate and to Silicone Surfaces. *Biomaterials* **2002**, *23*, 1495–1502.
- (17) Luo, L.; Li, G.; Luan, D.; Yuan, Q.; Wei, Y.; Wang, X. Antibacterial Adhesion of Borneol-Based Polymer via Surface Chiral Stereochemistry. *ACS Appl. Mater. Interfaces* **2014**, *6*, 19371–19377.
- (18) Shi, B.; Luan, D.; Wang, S.; Zhao, L.; Tao, L.; Yuan, Q.; Wang, X. Borneol-Grafted Cellulose for Antifungal Adhesion and Fungal Growth Inhibition. *RSC Adv.* **2015**, *5*, 51947–51952.
- (19) Chen, S.; Yuan, L.; Li, Q.; Li, J.; Zhu, X.; Jiang, Y.; Sha, O.; Yang, X.; Xin, J. H.; Wang, J.; Stadler, F. J.; Huang, P. Durable Antibacterial and Nonfouling Cotton Textiles with Enhanced Comfort via Zwitterionic Sulfopropylbetaine Coating. *Small* **2016**, *12*, 3516–3521.
- (20) Chen, Y.; Li, J.; Li, Q.; Shen, Y.; Ge, Z.; Zhang, W.; Chen, S. Enhanced Water-Solubility, Antibacterial Activity and Biocompatibility upon Introducing Sulfobetaine and Quaternary Ammonium to Chitosan. *Carbohydr. Polym.* **2016**, *143*, 246–253.
- (21) Chen, S.; Chen, S.; Jiang, S.; Xiong, M.; Luo, J.; Tang, J.; Ge, Z. Environmentally Friendly Antibacterial Cotton Textiles Finished with Siloxane Sulfopropylbetaine. *ACS Appl. Mater. Interfaces* **2011**, *3*, 1154–1162.
- (22) Quan, K.; Li, G.; Luan, D.; Yuan, Q.; Tao, L.; Wang, X. Black Hemostatic Sponge Based on Facile Prepared Cross-Linked Graphene. *Colloids Surf., B* **2015**, *132*, 27–33.
- (23) Li, G.; Wang, X.; Tao, L.; Li, Y.; Quan, K.; Wei, Y.; Chi, L.; Yuan, Q. Cross-Linked Graphene Membrane for High-Performance Organics Separation of Emulsions. *J. Membr. Sci.* **2015**, *495*, 439–444.
- (24) Zhao, Y.; Yu, Y.; Zhang, Y.; Wang, X.; Yang, B.; Zhang, Y.; Zhang, Q.; Fu, C.; Wei, Y.; Tao, L. From Drug to Adhesive: A New Application of Poly(dihydropyrimidin-2(1H)-one)s via the Biginelli Polycondensation. *Polym. Chem.* **2015**, *6*, 4940–4945.
- (25) Rasool, K.; Helal, M.; Ali, A.; Ren, C. E.; Gogotsi, Y. Antibacterial Activity of Ti₃C₂T_x MXene. *ACS Nano* **2016**, *10*, 3674–3684.
- (26) Jiang, J.; Zhu, L.; Zhu, L.; Zhang, H.; Zhu, B.; Xu, Y. Antifouling and Antimicrobial Polymer Membranes Based on Bioinspired Polydopamine and Strong Hydrogen-Bonded Poly(*N*-vinyl pyrrolidone). *ACS Appl. Mater. Interfaces* **2013**, *5*, 12895–12904.
- (27) Huang, S. C.; Hsieh, K. M.; Chang, T. W.; Chen, Y. C.; Yu, C. T. R.; Lu, T. C.; Lin, C. F.; Yu, T. Y.; Wang, T. T.; Chen, H. ZnO Nanoflakes on Silver Wires with Antibacterial Effects. *Ceram. Int.* **2016**, *42*, 7848–7851.
- (28) Cheng, L.; Weir, M. D.; Xu, H. H. K.; Antonucci, J. M.; Kraigsley, A. M.; Lin, N. J.; Lin-Gibson, S.; Zhou, X. Antibacterial Amorphous Calcium Phosphate Nanocomposites with a Quaternary Ammonium Dimethacrylate and Silver Nanoparticles. *Dent. Mater.* **2012**, *28*, 561–572.
- (29) Yeroslavsky, G.; Girshevitz, O.; Foster-Frey, J.; Donovan, D. M.; Rahimipour, S. Antibacterial and Antibiofilm Surfaces through Polydopamine-Assisted Immobilization of Lysostaphin as an Antibacterial Enzyme. *Langmuir* **2015**, *31*, 1064–1073.
- (30) Huang, C.; Chu, S.; Wang, L.; Li, C.; Lee, T. R. Bioinspired Zwitterionic Surface Coatings with Robust Photostability and Fouling Resistance. *ACS Appl. Mater. Interfaces* **2015**, *7*, 23776–23786.
- (31) Jiang, S.; Cao, Z. Ultralow-Fouling, Functionalizable, and Hydrolyzable Zwitterionic Materials and Their Derivatives for Biological Applications. *Adv. Mater.* **2010**, *22*, 920–932.
- (32) Kim, M. S.; Ahn, H. H.; Shin, Y. N.; Cho, M. H.; Khang, G.; Lee, H. B. An in Vivo Study of the Host Tissue Response to Subcutaneous Implantation of PLGA-and/or Porcine Small Intestinal Submucosa-Based Scaffolds. *Biomaterials* **2007**, *28*, 5137–5143.
- (33) Sun, K. H.; Liu, Z.; Liu, C.; Yu, T.; Shang, T.; Huang, C.; Zhou, M.; Liu, C.; Ran, F.; Li, Y.; Shi, Y.; Pan, L. Evaluation of *in Vitro* and *in Vivo* Biocompatibility of a Myo-Inositol Hexakisphosphate Gelled Polyaniline Hydrogel in a Rat Model. *Sci. Rep.* **2016**, *6*, 23931.
- (34) Movahedi, A.; Zhang, J.; Kann, N.; Moth-Poulsen, K.; Nyden, M. Copper-Coordinating Polymers for Marine Anti-Fouling Coatings:

A Physicochemical and Electrochemical Study of Ternary System of Copper, PMMA and Poly(TBTA). *Prog. Org. Coat.* **2016**, *97*, 216–221.

(35) Tang, Z. W.; Ma, C. Y.; Wu, H. X.; Tan, L.; Xiao, J. Y.; Zhuo, R. X.; Liu, C. J. Antiadhesive Zwitterionic Poly-(Sulphobetaine Methacrylate) Brush Coating Functionalized with Triclosan for High-Efficiency Antibacterial Performance. *Prog. Org. Coat.* **2016**, *97*, 277–287.

(36) Yang, C.; Ding, X.; Ono, R. J.; Lee, H.; Hsu, L. Y.; Tong, Y. W.; Hedrick, H.; Yang, Y. Y. Brush-Like Polycarbonates Containing Dopamine, Cations, and PEG Providing a Broad-Spectrum, Antibacterial, and Antifouling Surface via One-Step Coating. *Adv. Mater.* **2014**, *26*, 7346–7351.

(37) Tan, M.; Wang, H.; Wang, Y.; Chen, G.; Yuan, L.; Chen, H. Recyclable Antibacterial Material: Silicon Grafted with 3, 6-O-Sulfated Chitosan and Specifically Bound by Lysozyme. *J. Mater. Chem. B* **2014**, *2*, 569–576.

(38) Wu, H. X.; Tan, L.; Tang, Z. W.; Yang, M. Y.; Xiao, J. Y.; Liu, C. J.; Zhuo, R. X. Highly Efficient Antibacterial Surface Grafted with a Triclosan-Decorated Poly(n-Hydroxyethylacrylamide) Brush. *ACS Appl. Mater. Interfaces* **2015**, *7*, 7008–7015.

(39) Hu, W.; Peng, C.; Luo, W.; Lv, M.; Li, X.; Li, D.; Huang, Q.; Fan, C. Graphene-Based Antibacterial Paper. *ACS Nano* **2010**, *4*, 4317–4323.